13th World Conference on Earthquake Engineering
Vancouver, B.C., Canada
August 1-6, 2004
Paper No. 1893

# DYNAMIC RESPONSE ANALYSIS OF LARGE AQUEDUCT TO EARTHQUAKE GROUND EXCITATIONS

**Wenyi Chen[1] and Hong Hao[2]**

## SUMMARY

Almost every year south China in the Yangtze river catchments area floods, while at the same time water ration policy sometimes has to be implemented in north China because of drought. As such, engineers and policy makers in China have been dreaming for canals to divert water from South to North for many years. Since the project requires huge investment, and possibly causes some environmental problems, only recently the project has finally reached the planning and designing stage. However, feasibility studies and research work has never stopped for the last five decades. It has been decided that three canals will be constructed from south to north, namely west route, middle route and east route. When crossing existing rivers running from west to east, either under-river tunnels or elevated aqueducts will be built.

In this study, seismic response analysis of a proposed aqueduct in the middle route crossing a seismic zone in north China will be performed. Particular effort is devoted to find a suitable numerical model that can accurately represent the proposed aqueduct design, water-structure interaction, and the effects of bearing properties of the aqueduct supports on its responses to seismic ground excitation. SAP2000 Computer program is used in the analysis. Numerical model is validated by comparing the simulated results with independently obtained test results. Spatially varying seismic ground motions are stochastically simulated and used as input in the analysis. The simulated ground motion time histories are compatible with the design spectrum specified in the Chinese Seismic Design Code for the area under consideration. It is found that using isolated bearing in the design can significantly reduce the aqueduct responses, as

[1] Gledden Fellow, School of Civil and Resource Engineering, The University of Western Australia, on leave from Department of Civil Engineering, North China Institute of Water Conservancy and Hydroelectric Power, email: chen_wyi@sohu.com
[2] Associate Professor, School of Civil and Resource Engineering, The University of Western Australia, 35 Stirling Highway, Crawley, WA 6009, Australia, email: hao@civil.uwa.edu.au

compared to the hinge support design option. However, the lateral stiffness of the bearing should be properly designed to avoid resonance between the aqueduct and water mass in the aqueduct.

## INTRODUCTION

The disaster caused by flood in the Yangtze river catchments area in south and central China occurs almost every year and it has resulted in millions of dollars in economic losses and in some years claimed hundreds of lives. At the same time, water ration some times has to be enforced in north China because of frequent drought. Engineers in China have been dreaming for a long time of building canals to divert water from Yangtze river catchments area to north China. Feasibility studies started in early 1950's and has been on and off for more than 50 years depending on country's political and economical situations. It was until December 2002 that the Chinese government finally launched the project.

Three water diversion canals will be constructed, namely west, middle and east route from south to north. The middle route starts from Danjiankou reservoir in Hubei province in Central China with a total length of 1241 km and will provide 13 to 14 billion cubic meters of water supply annually to Beijin and Tianjin Metropolitan areas after the construction finished in 2030, as shown in Figure 1. Some design work has been carried out. The canal will across many rivers on its way north. Either under-river tunnels or elevated aqueducts will be constructed.


Fig. 1 Planned middle route of south-north water diversion canal
(from http://www.water-technology.net/projects/south-north/ )

In this study, numerical analysis of seismic responses of an elevated aqueduct will be carried out. The preliminary design of the aqueduct had been completed without performing rigorous seismic response analysis besides applying equivalent static forces in the design, although shaking table tests of a 1:20 scaled model had been carried out. The aqueduct is located in the Chinese seismic intensity zone 7. Owing to the importance of the aqueduct, however, it was decided to design it using seismic forces specified for seismic zone 8 with a design PGA of 70 cm/s$^2$ for normal operating condition and 400 cm/s$^2$ for extreme conditions, China Ministry of Construction [1]. In this study, the seismic ground motion time histories for normal operating condition are simulated for the analysis.

The aqueduct has a cross section of 27.5×9.45 m, and is elevated 21.68 m above the ground on RC piers, each span length is 40 m. Other researchers had performed shaking table tests on a one-span 1:20 scale model with or without water in the aqueduct Hu [2]. Those testing data will be used to verify the accuracy of the present numerical model. The study will analyze the following: 1) minimum number of spans that should be included in the numerical model to reach an accurate estimation; 2) methodologies of modeling water in the aqueduct and the effects of water mass on aqueduct responses; 3) properties of supporting conditions of the aqueduct on piers, namely rubber bearing or hinge support on dynamic responses; 4) properties of the infill materials in expansion joints on pounding responses; 5) pounding between adjacent spans; and 6) earthquake ground motion spatial variability on aqueduct responses. Spatial Ground motion time histories will be stochastically simulated according to the design response spectrum specified in the current Chinese Seismic Design Codes, China Ministry of Construction [1], and an empirical ground motion spatial variation functions Hao [3]. In this paper, discussions are made on modeling of water-structure interaction and the effects of bearing properties on the aqueduct responses. Only the results obtained based on analyzing a single span is presented. The effects of ground motion spatial variation, effects of pounding between adjacent spans, and the effects of infill materials in the expansion joints on dynamic responses of aqueduct to seismic ground excitations will be presented in the future.

## AQUEDUCT MODEL

The aqueduct analyzed in this study is named Minhe Aqueduct. It is located in the southern part of Hebei province in China. The total length of the aqueduct is 680 m, consisting of 17 spans with a constant span length of 40 m. The cross section dimension of the aqueduct is 27.5×9.45 m. It consists of four longitudinal prestressed RC beams of dimension 8.65×0.7 m. The four beams divide the aqueduct into three channels each with a width of 8.3 m and a height of 7.0 m. The operating water depth is designed to be 5.74 m, with the total water weight of 5717 t on each span. The four prestressed beams rest on hollow piers of height 21.68 m, and bottom dimension 35×9 m.  Figure 2 shows the Minhe aqueduct.

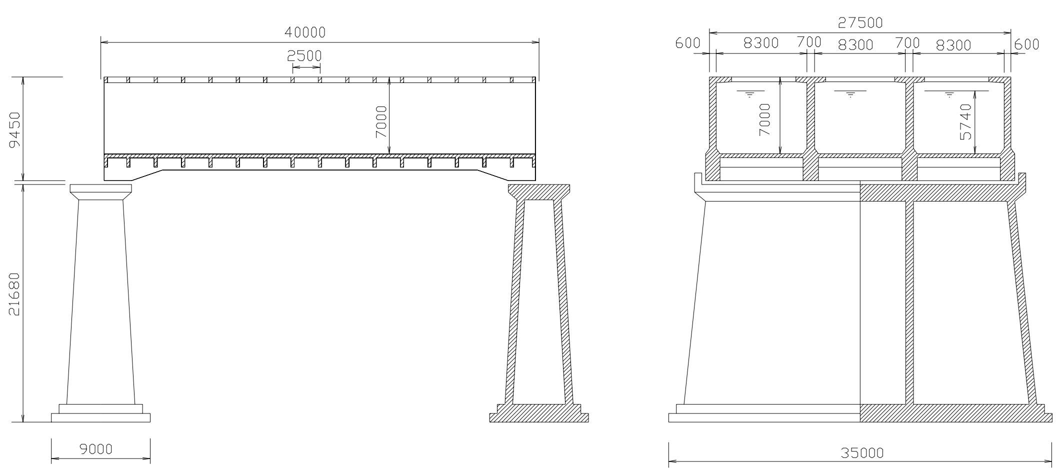


Fig. 2 Minhe Aqueduct

On top of each beam, there is a 2.0 m flange. This flange increases the stiffness of the beam, and at the same time will be used as walkway in the future. The flanges of the four beams are linked together transversely at a longitudinal spacing of 2.5 m by a beam. Transverse stiffeners are also provided on the bottom plate of the aqueduct, also at a longitudinal spacing of 2.5 m. Initially the aqueduct was designed to be hinge supported on the piers. Therefore, the scaled model tested on shaking table was hinge supported. At a later stage, isolating bearing supports were suggested to reduce the seismic actions on the aqueduct structure. But no design on the bearing supports has been performed yet.

## NUMERICAL MODEL

### Structural model

The commercial software package SAP2000, CSI [4], is used for numerical analysis. The structure is modeled by beam and plate elements. Beam elements are used to model the bars on top of the aqueduct connecting the four main prestressed beams. The aqueduct and the hollow piers are modeled by plate elements. The material properties and dimensions of the aqueduct structure as used in the design are adopted in the numerical model. In the preliminary design stage, the aqueduct was designed to be hinge supported on piers. Shaking table tests of a 1:20 scaled one-span aqueduct model were carried out. In a later stage, it was decided to use rubber bearing to isolate the aqueduct from the piers in order to reduce the seismic actions on the structure. In the present study, to verify the accuracy of the numerical model, responses of the aqueduct with hinge supports are calculated first and compared with the tests results. To study the effects of different bearing supports on reducing the seismic responses of the aqueduct, numerical analyses of the dynamic responses of aqueduct with rubber bearing supports of different lateral stiffness are performed. The results are compared with each other and are also compared with those obtained with hinge supports. An optimal choice of the bearing lateral stiffness can be derived from the numerical results. Figure 3 shows the force-displacement relations used in the numerical model for rubber bearing. A typical rubber bearing has an initial horizontal shear stiffness 2.0t/mm, and the yield shear strength 10t. The post yield stiffness is 10% of the original stiffness. The rubber bearing is 250 mm thick. In numerical calculations, the initial stiffness $k_e$ is varied to study its effect on aqueduct-water interaction.

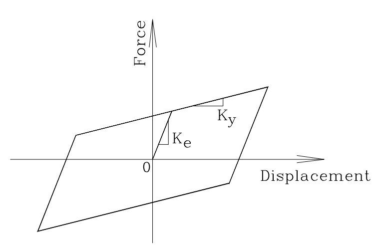


Fig. 3 Force-displacement relation of the rubber bearing support

### Water model

Various numerical methods have been developed to model water-structure interaction, for example, Fok [5]. Those methods are either based on finite element method or boundary element method. They were proven yielding reliable estimation of water vibrations and water-structure interaction. Their applications are, however, very complicated and usually associated with some specific computer programs Fok [5]. In this study the simple and yet reliable method developed by Housner [6, 7] is employed to model water-aqueduct interaction.

Housner's method divides dynamic water pressure on aqueduct wall into two parts, namely the impulsive and convective pressure. The impulsive pressure is assumed to be independent of the water vibration mode inside the aqueduct. It is equivalent to a static water mass attaching to the structure and vibrating exactly in-phase with the aqueduct wall, as shown in Figure 4(a), in which $M_0$ is the equivalent impulsive mass and $H_0$ its equivalent height. $M_0$ and $H_0$ are estimated by the condition that it results in the same bending moment at the bottom of the aqueduct wall as the impulsive pressure.

The convective pressure is produced on the aqueduct wall because of water vibration inside the aqueduct. It depends on the water vibration properties and is modeled by an equivalent mass $M_i$ and stiffness $K_i$ for the ith water vibration mode. Because convective pressure from high water vibration modes are very small as compared with the impulsive pressure, usually only the first convective mode is considered. Figure 4(a) also shows the equivalent convective mass $M_1$, which is connected to the aqueduct wall with an equivalent spring of stiffness $K_1$ at an equivalent height $H_1$.

The equivalent mass and height for the convective pressure are, Housner [6,7]

$$M_0 = \frac{\tanh(\sqrt{3}l/H)}{\sqrt{3}l/H} M \tag{1}$$

and $H_0=3/8H$, where $2l$ is the width of the aqueduct, $H$ is the water depth, and $M=2\rho_W lH$ is the total water mass.

The equivalent convective vibration parameters of water mass are, Housener [6,7]

$$M_1 = \frac{1}{3}\sqrt{\frac{5}{2}}\frac{l}{H}\tanh(\sqrt{\frac{5}{2}}\frac{H}{l})M \tag{2}$$

$$H_1 = H[1 - \frac{1}{\sqrt{\frac{5}{2}}\frac{H}{l}\tanh(\sqrt{\frac{5}{2}}\frac{H}{l})}] \tag{3}$$

and the water vibration circular frequency and equivalent stiffness are

$$\omega = [\sqrt{\frac{5}{2}}\frac{g}{l}\tanh(\sqrt{\frac{5}{2}}\frac{H}{l})]^{1/2} \tag{4}$$

$$K_1 = 3\frac{M_1^2}{M}\frac{gH}{l^2} \tag{5}$$

in which $g$ is the gravity constant.

In numerical modeling, if two concentrated masses $M_0$ and $M_1$ are directly applied to the aqueduct wall at their respective equivalent height as shown in Figure 4(a), it results in large stress concentrations at the corresponding points. To avoid this, the two equivalent masses as well as the equivalent stiffness for convective pressure are distributed along the height of the wall according to the respective pressure distribution, as shown in Figure 4(b). In Hournser's model, the impulsive pressure acting on the container wall is estimated by

$$p(y) = \rho_W H\sqrt{3}[y/H - 0.5(y/H)^2]\tanh(\sqrt{3}l/H) \tag{6}$$

and the convective pressure by

$$p(y) = \rho_W \frac{l^2}{3}\sqrt{\frac{5}{2}}\frac{\cosh(\sqrt{\frac{5}{2}}\frac{y}{H})}{\sinh(\sqrt{\frac{5}{2}}\frac{y}{H})}\omega^2\theta_h \sin\omega t \tag{7}$$

where $y$ is as shown in Figure 4(a) and $\theta_h$ is the largest oscillation angle of the water surface at $y=0.0$.

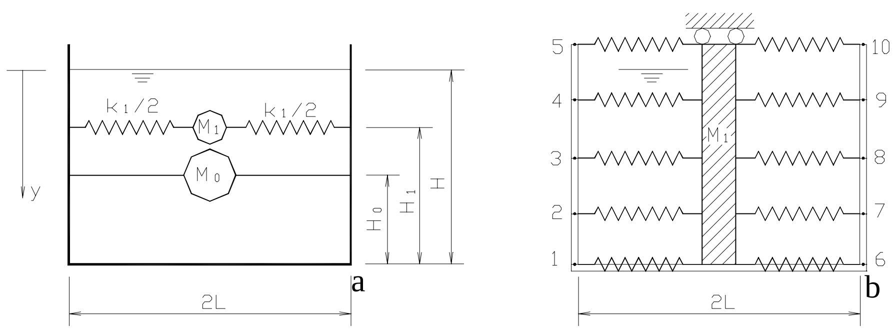


Fig. 4 Housner's equivalent impulsive and convective mass and stiffness of water pressure

It should be noted that the convective mode, that is the water mass vibration, also produces vertical pressure on the bottom plate of the aqueduct. However, this dynamic pressure is relatively small as compared with the static water pressure on the aqueduct bottom plate. In this study, this vertical dynamic pressure is neglected. The vertical static pressure is included in the numerical model as additional mass on the bottom plate.

## SPATIAL EARTHQUAKE GROUND MOTION

Because of wave propagation, ground motions at different locations inevitably vary. Ground motion spatial variation properties depend on seismic source, wave path and local site conditions. In that study, spatial earthquake ground motions at the aqueduct piers are simulated, Hao [3]. Figure 5 shows the simulated ground acceleration time histories in the three directions. The simulations are performed by assuming that seismic wave propagation apparent velocity $v_a$ is 1000 m/s; separation distance between each point d=40 m; wave propagation direction coincides with the longitudinal direction of the aqueduct span; ground motion spatial variation properties are similar to the recorded motion during Event 45 at the SMART-1 array, Hao [3]; and ground motion intensity is compatible with the Chinese Seismic Design Code for zone 8, China Ministry of Construction [1].

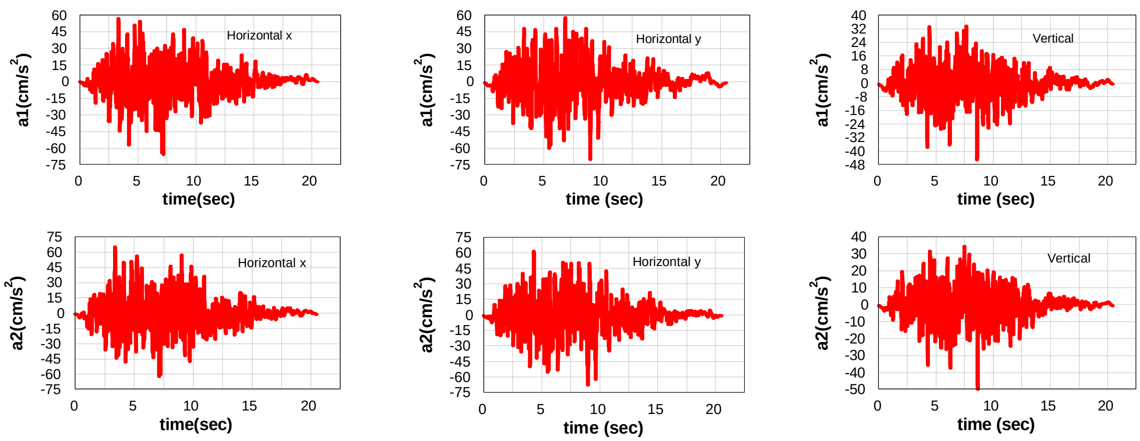


Fig. 5 Simulated spatial ground acceleration time histories

Figure 6 shows the corresponding ground displacement time histories. As shown, because motions at locations separated by a distance of 40 m are highly correlated, the simulated motions are very similar, but not the same.

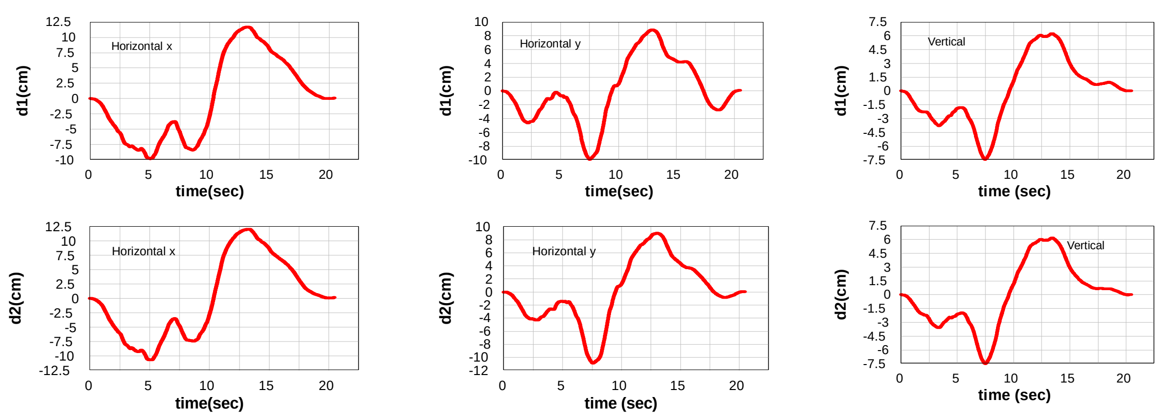


Fig. 6 Simulated ground displacement time histories

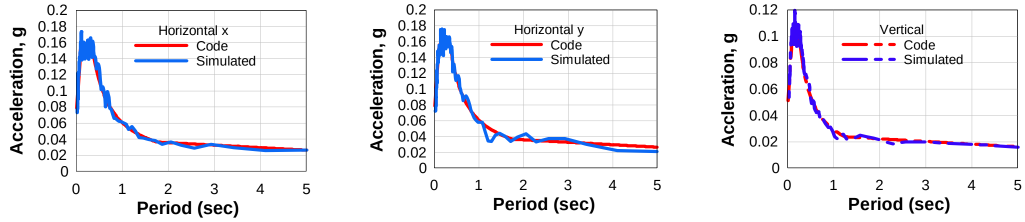


Fig. 7 Comparison of code design spectrum and those of the simulated ground motion

Figure 7 shows the comparison of the acceleration response spectrum of the simulated motion with the acceleration response spectrum specified in Chinese Seismic Design Code for zone 8 [1]. As shown, the simulated motion correlates very well with the target response spectrum.

Figure 8 shows the comparison of the coherency loss between simulated motions separated by 40 m and the empirical coherency loss function derived from recorded motion at the SMART-1 array during Event 45. Good agreement is observed.

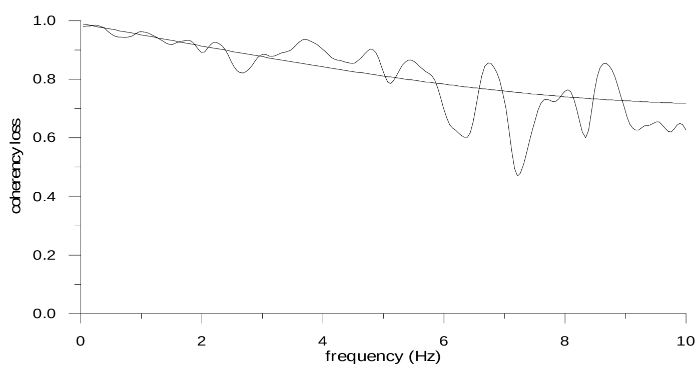


Fig. 8 Coherency loss of the simulated motion and empirical coherency loss function

The simulated spatial ground motion time histories will be used in the numerical calculation as input. More detailed information on ground motion simulation and spatial variation can be found in Hao [3].

## NUMERICAL MODEL VALIDATION

A 1:20 scaled aqueduct model with hinge support was tested on shaking table Hu [2]. The test results are used here to verify the accuracy of the numerical model. Table 1 gives a comparison of the measured prototype aqueduct vibration frequencies and those obtained from numerical simulation. As can be noticed, the numerical results matches reasonably well with the measured ones. It should be noted that the numerical model also gives that the first three vibration modes are water vibrations, with the vibration frequencies of 0.2905 Hz, 0.2910 Hz and 0.2910Hz. Because only the aqueduct vibration frequencies are measured in the tests, the water vibration frequencies are not listed in Table 1 for comparison.

**Table 1 Comparison of measured and calculated aqueduct vibration frequencies**

| Water level | Longitudinal (Hz) | | | Transverse (Hz) | | |
|---|---|---|---|---|---|---|
| | Test | Numerical | Error | Test | Numerical | Error |
| Empty | 2.64 | 2.70 | 2.3% | 4.73 | 3.95 | -16.5% |
| Full | 2.24 | 2.70 | 20.5% | 3.59 | 3.04 | -15.3% |

As shown, the largest error occurs in the first longitudinal vibration mode with full water condition. This is because there is no constraint of longitudinal water movement in the numerical model, but water in the testing model is fully contained in the one-span aqueduct. In reality, water is not constrained longitudinally, but it will not flow freely without any friction either as in the numerical model. Therefore, the actual vibration frequency should be somewhere between 2.24 Hz and 2.70 Hz. Because the effect of friction on longitudinal vibration frequency cannot be very significant, it is believed that the numerical result might be more accurate than the test one. The error on the transverse vibration frequencies might be attributed to the modeling of the beams connecting transversely on the top of the prestressed main aqueduct beams. Because no detailed design data are available yet for such transverse beams, the beam used in the testing model might not be the same as in the numerical model.

Figures 9 and 10 show the first few vibration modes of the one-span hinge supported aqueduct with empty and full water condition, respectively. These vibration modes are similar to those observed in the tests.

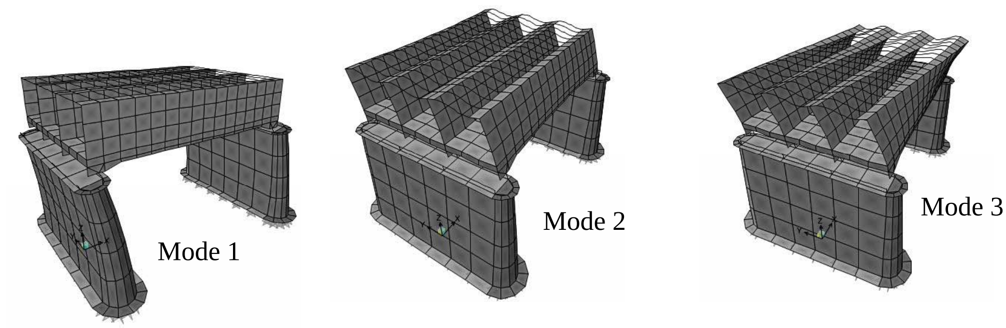


Fig. 9 The first three vibration mode shapes of the hinge supported empty aqueduct

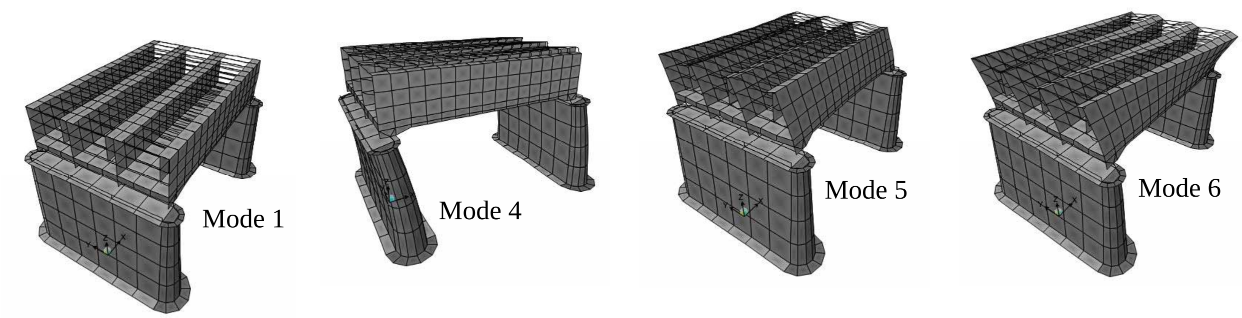

Fig. 10 The first and the fourth to the sixth vibration mode shapes of hinge supported aqueduct with full water

It should be noted that when there is water in the aqueduct, the first three vibration modes are associated with water mass vibration, ie, the convective mode of the water mass. The fourth to the sixth modes are aqueduct vibration, which are the same as the first three vibration modes of the empty aqueduct.

Numerical analysis also gives that under full water condition the largest tensile stress on the pier is 2.19 MPa, occurring at about 5 m above the ground. When the aqueduct is empty, the largest tensile stress on the pier is more or less the same because water in the aqueduct has little effect on the longitudinal responses of the aqueduct. This observation is similar to the testing results. Under full water condition, the largest stress on piers was measured as 2.4 MPa, and this value remains almost unchanged when reducing the water depth from H to 1/3H. The difference might be attributed to the condition that water was fully constrained in the test, as discussed above.

Under the full water condition, the largest longitudinal stress on the bottom plate of the aqueduct was measured as 2.0 MPa in the test, occurring at the mid span, while the numerical simulation gave 2.1 MPa. The largest transverse stress on the bottom plate was measured in the tests as 2.5 MPa at the mid span, and 5.0 MPa at the support, whereas they were 2.16 MPa and 3.73 MPa from numerical simulation. The largest error between the test and numerical results is the transverse stress near the support. In general the numerically simulated responses in the longitudinal direction are closer to the test results than in the transverse direction. This is probably because non-identical transverse beams and stiffeners on aqueduct were used in the test and numerical model as discussed above.

The above comparison and discussion demonstrated that the numerical model developed using SAP2000 gives reasonable prediction of aqueduct responses to seismic excitations.

## NUMERICAL RESULTS

As discussed above, rubber-bearing supports will most likely be used in actual construction, instead of hinge supports. In this section, responses of the aqueduct supported on rubber-bearing of different stiffness are calculated. Figure 11 shows the first three vibration mode shapes of the empty aqueduct.

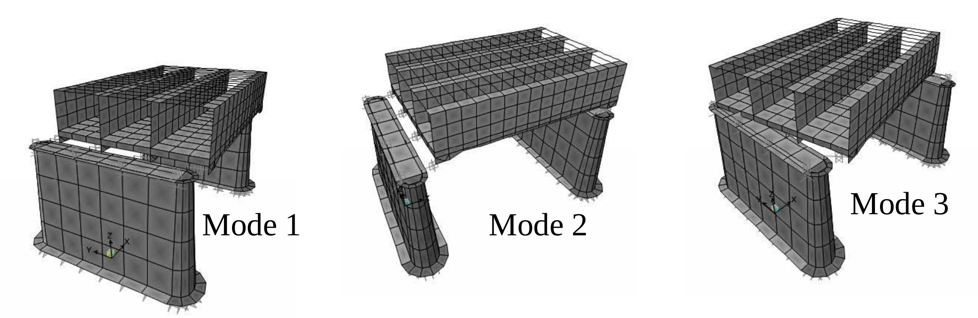

Fig. 11 The first three vibration mode shapes of the rubber-bearing supported empty aqueduct

As compared with those shown in Figure 9, the vibration mode shapes change completely. Now the first three modes are associated with the relative movement of the aqueduct channel above the piers. When the aqueduct is full of water, like in the hinge support case, the first three vibration modes are water mass vibration and the fourth to the sixth are the same as those shown in Figure 11.

Figure 12 shows the vibration periods of the aqueduct with empty and full water conditions as a function of the shear stiffness of the rubber bearing. The vibration period of the water mass is also shown in the figure. As shown, the vibration periods of the aqueduct decreases exponentially with the increase of the bearing stiffness. The vibration period of water mass is, however, almost independent of the bearing stiffness, but when $k_e \approx 4$ kN/mm, there is a sudden change in the vibration period of the aqueduct and water mass as indicated by a, b in the figure. This is caused by resonance of the water and aqueduct when their vibration periods are close to each other. When $k_e$=600 kN/mm, the vibration period converges to that of the hinge supported case.

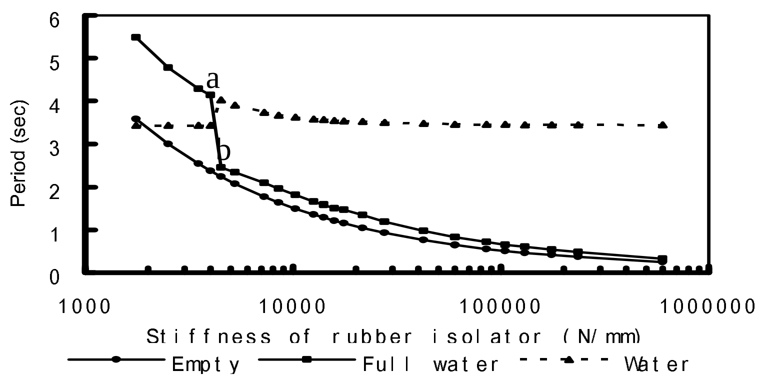


Fig. 12 Vibration period versus rubber-bearing shear stiffness

Figure 13 shows the largest vertical stress on the middle beam or partition wall of the aqueduct channel (M752), side beam (M848), and horizontal tensile stress at the bottom plate (M263) of the aqueduct. As shown, all the stresses reduce significantly by increasing the vibration period from 0.3788 sec (2.64 Hz, hinge support) to about 1.0 sec by using $k_e$=20 kN/mm. The stress at M848, M752 and M263 corresponding to the hinge supported case are 1.95 MPa, 2.78 MPa and 1.6 MPa, respectively; and are reduced to about 0.5 MPa, 0.6 MPa and 0.4 MPa when vibration period is about 1.0 sec. Further increase the vibration period will still reduces the responses, but the effect is not very significant. Points a, b in the figure correspond to those shown in Figure 12, and point c corresponds to the minimum stress.

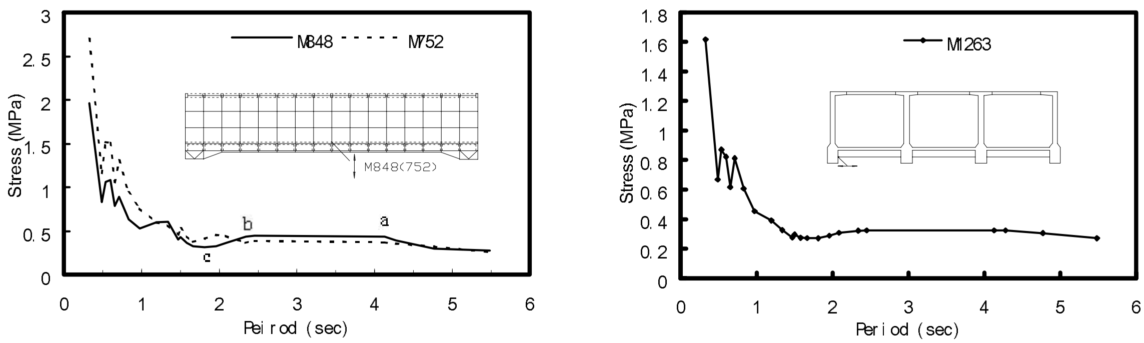


Fig. 13 Stress reduction as a function of vibration period

It should be noted that the current numerical results were obtained without considering pounding between adjacent spans. With rubber-bearing supports, the relative displacement of channels will be large and pounding might occur, which will change the stresses in the structure.

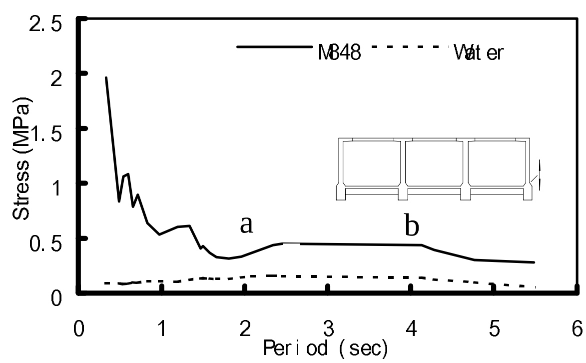


Fig. 14 Significance of water vibration generated stress

Figure 14 shows the vertical stress at point M848 and the corresponding stress produced by water vibration in the aqueduct. As shown, when the aqueduct is hinge supported, the stress induced by water vibration is only 0.09 MPa, as compared to the 1.95 MPa. The stress induced by water vibration is negligible. However, when the vibration periods of water mass and aqueduct are close to each other (in portion a-b), the stress induced by water mass vibration is 0.16 MPa, which is 36% of the total stress in the structure. This observation indicates that the effects of water vibration can be neglected in the analysis and design when the aqueduct is hinge supported. Water mass can be considered as additional mass on the aqueduct structure, or only the impulsive mass needs be included. When aqueduct is rubber-bearing supported with relatively small vibration frequency, however, the vibration mode of the aqueduct might resonate with that of water mass. In that case, the convective mode of the water vibration cannot be neglected in the analysis.

Figure 15 shows the vertical stress time histories at point M848 corresponding to different vibration period of the aqueduct with hinge supports or bearing supports. It shows clearly that the stress induced by water mass vibration (convective mode) might become very significant.

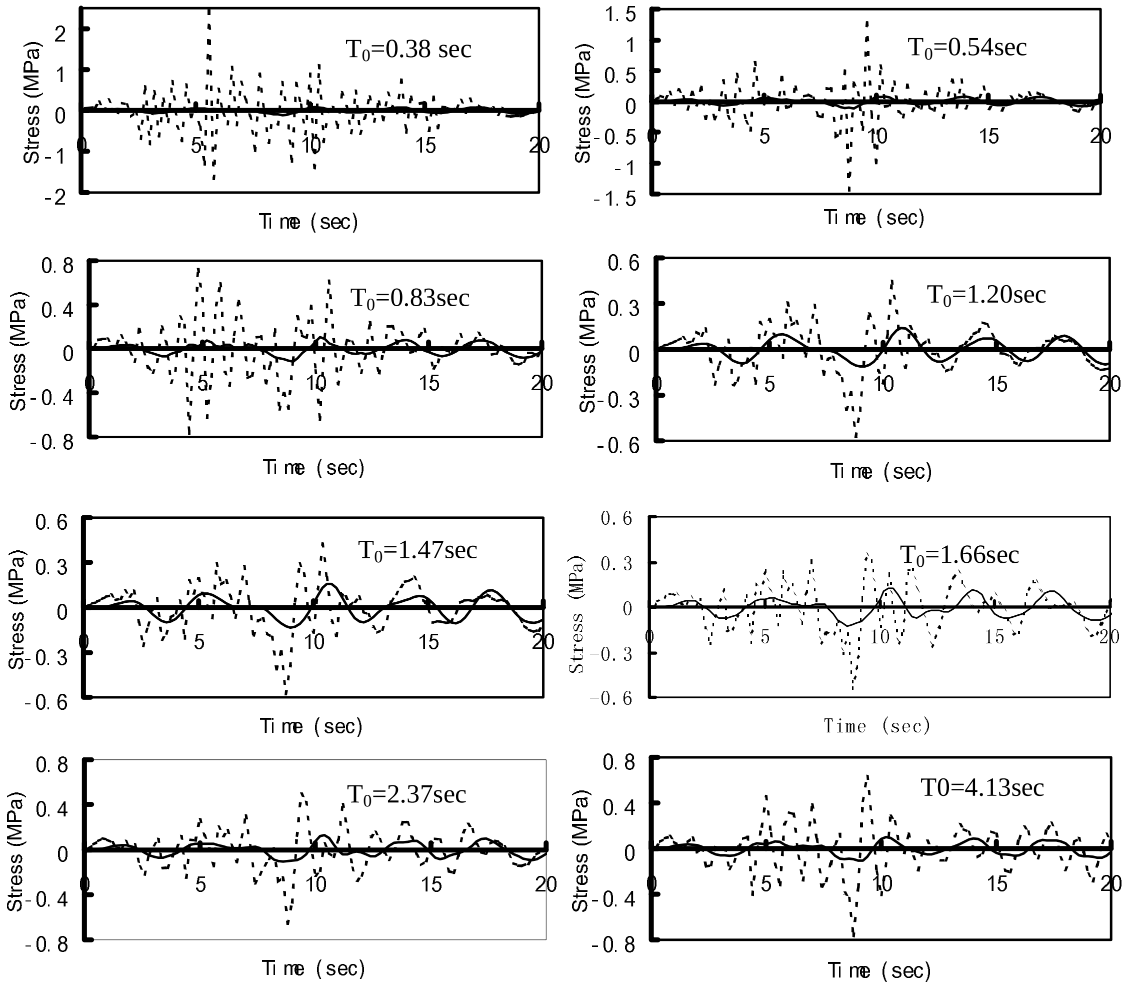


Fig. 15 Stress time histories at point M848
( ------------ total stress; ———— Stress induced by water vibration)

## CONCLUSIONS

Many aqueducts in the three routes of south-north water diversion project will be similarly designed as Minhe aqueduct analyzed in this study. Thus it is very important to establish a reliable numerical model for seismic response analysis. The numerical model developed using SAP2000 in this study was proven yielding accurate predictions of aqueduct vibration properties and dynamic responses.

This study also demonstrated that using bearing supports would greatly reduce aqueduct responses to seismic ground motion as compared to using hinge supports. Reducing the stiffness of the bearing supports reduces the responses. However, it is effective only when the shear stiffness of the bearing supports is about 30 kN/mm, further reduction of the bearing stiffness does not have a significant effect on reducing aqueduct responses, but has a potential of resulting in resonance between aqueduct and water mass, which will increase slightly the aqueduct responses. Moreover, if the bearing stiffness is very small, the longitudinal displacement of the aqueduct channel will be large and this will substantially increase the pounding potentials between adjacent aqueduct spans. Therefore an optimal bearing stiffness needs be determined in the design of isolated aqueduct. The study also found that if the aqueduct is relatively stiff (hinge supported), the effect of convective mode of water vibration on aqueduct is insignificant and water inside the aqueduct channel can be considered as a static mass in the analysis. When aqueduct vibration mode is close to that of water vibration, the contribution from water vibration (convective mode) cannot be neglected.

## ACKNOWLEDGEMENT

The first author was partially supported by the Gledden Fellowship of the University of Western Australia for his one-year stay in Australia. This support is greatly appreciated.

## REFERENCES

1. Ministry of Construction, “Code for seismic design of buildings: GB50011-2001”, Ministry of Construction, People’s Republic of China, Beijing, 2001.
2. Hu X, Wang J,Yu Y, Wei L, Wang QZ and Zhou AL, “Experimental study of seismic response of Minhe Aqueduct in middle route of south-north water diversion project”, Earthquake Engineering Research Center, China Hydraulic and Hydropower Research Institute, Beijing, 2002.
3. Hao H, “Effects of spatial variation of ground motions on large multiply-supported structures”, Report No. 89-06, Earthquake Engineering Research Center, University of California at Berkeley, 1989.
4. Computers and Structures Inc. (CSI), “SAP2000 –Version 8, Analysis Reference Manual”, 1995 University Ave., Berkeley, CA 94704, USA, 2002.
5. Fok KL, Hall, JF and Chopra AK, “ECAD-3D: A computer program for three-dimensional earthquake analysis of concrete dams”, Report No. EERC86-10, Earthquake Engineering Research Center, University of California at Berkeley, 1986.
6. Housner GW, “The dynamic behaviour of water tanks”, Bull. of Seis. Soc. of Am, Vol. 53(1), 1963, pp381-387.
7. Housner GW, “Dynamic pressure on accelerated fluid containers”, Bull. of Seis. Soc. of Am, Vol. 47(1), 1957, pp15-35.